

Spin-polarization of (Ga,Mn)As measured by Andreev Spectroscopy: The role of spin-active scattering

S. Piano,¹ R. Grein,² C. J. Mellor,¹ K. Vyborny,³ R. Campion,¹ M. Wang,¹ M. Eschrig,^{2,4,5} and B. L. Gallagher¹

¹*School of Physics and Astronomy, University of Nottingham,
University Park, Nottingham, NG7 2RD, United Kingdom*

²*Institut für Theoretische Festkörperphysik and DFG-Center for Functional Nanostructures,
Karlsruhe Institute of Technology, D-76128 Karlsruhe, Germany*

³*Institute of Physics ASCR, v.v.i., Cukrovarnická 10, Praha 6, CZ-16253, Czech Republic*

⁴*Fachbereich Physik, Universität Konstanz, D-78457 Konstanz, Germany*

⁵*SEPnet and Hubbard Theory Consortium, Department of Physics, Royal Holloway,
University of London, Egham, Surrey TW20 0EX, United Kingdom*

(Dated: February 18, 2011)

We investigate the spin-polarization of the ferromagnetic semiconductor (Ga,Mn)As by point contact Andreev reflection spectroscopy. The conductance spectra are analyzed using a recent theoretical model that accounts for momentum- and spin-dependent scattering at the interface. This allows us to fit the data without resorting, as in the case of the standard spin-dependent Blonder-Tinkham-Klapwijk (BTK) model, to an effective temperature or a statistical distribution of superconducting gaps. We find a transport polarization $P_C \approx 57\%$, in considerably better agreement with the $\vec{k} \cdot \vec{p}$ kinetic-exchange model of (Ga,Mn)As, than the significantly larger estimates inferred from the BTK model. The temperature dependence of the conductance spectra is fully analyzed.

PACS numbers: 72.25.Mk, 74.45.+c, 75.50.Pp

The quickly evolving field of spintronics, which addresses the manipulation and exploitation of the quantum-mechanical spin of an object, has led to an intense search for spin-polarized materials as promising candidates for applications. Current metal spintronic devices and most proposed semiconductor spintronic devices aim to exploit the net spin-polarization (SP) of charge carriers to encode and/or process information. The advantage of using ferromagnetic (FM) semiconductors is their potential to serve as spin-polarized carrier sources and the possibility to easily integrate them into semiconductor devices¹. Recently, the family of (III,Mn)V FM semiconductors has attracted much attention for their potential usage in non-volatile memory, spin-based optoelectronics and quantum computation². In particular, (Ga,Mn)As, with a Curie temperature as high as 185 K^{3,4} is one of the most prominent materials for such applications.

The degree of SP is the key parameter for most spintronic functionalities. The injection of spin-polarized currents from FM semiconductors into nonmagnetic semiconductor devices has been demonstrated by measurements of the optical polarization of light emitted after recombination of spin-polarized holes with electrons in nonmagnetic semiconductors⁵. However, the resulting polarization is strongly dependent on the experimental set-up and the spin relaxation rate in the nonmagnetic part of the device, so that it is very difficult to infer reliable values of SP from such measurements⁶. Specialized techniques based on superconductor (SC)/FM junctions have been employed frequently in recent years to obtain information on the SP in metals^{7,8}. In particular, the point contact Andreev reflection (PCAR) technique has become a popular tool to measure the transport SP P_C of carriers at the Fermi level in FM materials^{9,10}. The PCAR data contains information regarding the carrier SP because the Andreev reflection process is spin-sensitive. Andreev reflection is the only allowed process of charge transfer across a contact between a

SC and a normal metal at energies below the SC gap. In this process, a Cooper pair is created in the SC when a quasiparticle tunnels from the normal metal and a hole is reflected back coherently. Two particles with opposite spin are in fact transferred, hence the probability of this process is reduced when the density of states for spin- \uparrow/\downarrow carriers is different. This results in a suppression of the conductance for voltages below the SC gap and thus the degree of SP can be estimated from such conductance spectra^{11,12}. However, the reliability of the P_C -values obtained with this technique — based on fitting the spectra to an extension of the Blonder-Tinkham-Klapwijk (BTK) model^{11,13} — is currently under debate^{8,14-16}.

Here we present a detailed PCAR study of the carrier (hole) SP in (Ga,Mn)As. The measurements have been carried out at different temperatures starting from about 2K up to the point where the SC gap in the tip closes. The shape of the experimental conductance spectra shows a suppression of the conductance for voltages smaller than the SC gap and a complete absence of coherence peaks at the gap edge. However, in agreement with earlier PCAR measurements on this material, the conductance suppression below the gap energy is rather small, with a minimum of about 0.7 G_N , where G_N is the conductance in the normal state. This feature would usually hint at an intermediate SP of the FM-material. Yet, if one tries to fit these spectra with the BTK theory, it turns out that the two key features, the absence of coherence peaks and the rather high zero-bias conductance, cannot be reconciled within this model. To remedy this situation, one needs to appeal to an “effective” fictitious temperature, T^* , which we find to be almost 6 times as high as the real sample temperature in our case. With this additional fit parameter, satisfactory fits can be achieved extracting a high value of P_C ($\gtrsim 90\%$).

We propose a more sensible interpretation of the data using a model of interface scattering that goes beyond the BTK theory, showing that an excellent agreement can be achieved

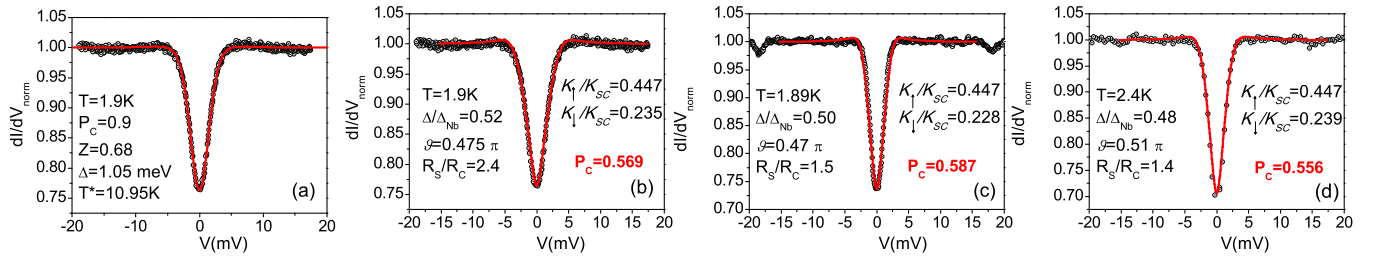


FIG. 1: (Color online) Experimental PCAR data (black dots) for the as-grown sample together with the theoretical fit (red line), (a) using the modified BTK model, (b) according to the spin-active scattering (SAS) model in Ref.¹⁴. (c) Annealed sample and (d) another PCAR probe applied to the as-grown sample, both analyzed using the SAS model. The fitting parameters are in the caption of the Figs. We emphasize that the temperature (T) and the value of the transport SP P_C in Figs. (b), (c) and (d) are not fitting parameters, as explained in the text.

without an effective temperature. From this analysis we infer a value of the SP of about 57%. The expected range of P_C is moreover analyzed with the $\vec{k} \cdot \vec{p}$ exchange model, providing further confirmation that the BTK SP value was far from realistic. We also notice a substantial reduction of the SC energy gap and critical temperature of the Nb tip, probably related to an inverse magnetic proximity effect. From measurements of the conductance spectra at different temperatures, we extrapolate the temperature dependence of the energy gap.

We have investigated 7% Mn doped, 25nm thick (Ga,Mn)As samples. They are grown on a 400nm thick, highly carbon-doped ($\approx 10^{19}\text{cm}^{-3}$) buffer layer to minimise series resistance. The Curie temperature T_C is $\approx 70\text{K}$ for the as-grown sample and $\approx 140\text{K}$ after 24 h of annealing at 190°C . The details of the sample growth and preparation are described elsewhere¹⁷. The experiments were carried out by means of a variable temperature (1.5–300 K) cryostat. Sample and Nb tip (chemically etched) were introduced into the PCAR probe, in which a piezo motor and scan tube can vary the distance between tip and sample. The PCAR junctions were formed by pushing the Nb tip on the (Ga,Mn)As surface with the probe thermalized in ^4He gas. The current-voltage I vs V characteristics were measured by using a conventional four-probe method and, by using a small ac modulation of the current, a lock-in technique was used to measure the differential conductance dI/dV vs V .

In Fig. 1 we show conductance spectra at low temperature ($T \approx 2\text{K}$), the resistance at high bias (that corresponds to the resistance of the normal state) for the different contact was about $28 - 30\ \Omega$. The data of Fig. 1(a) and (b) is identical, but (a) is fitted with the extended BTK model and b-d with the theory of¹⁴. The data has been normalized using the background conductance estimated at large voltage ($V \gg \Delta_{\text{Nb}}/e$) regions, where $\Delta_{\text{Nb}} \approx 1.5\text{meV}$ is the SC gap of Nb. All conductance spectra show a moderate dip and completely suppressed coherence peaks at the gap edge. While different PCAR probes on the same sample, Fig. 1(b,d), result in different point-contact resistances R_{pc} , the fitted value of P_C is almost constant. No significant difference in the spectra (and P_C) has been noticed before and after annealing as shown in Fig. 1(b–d), which is remarkable given that such annealing reduces the resistivity by a factor of ~ 2 in these samples due to the large increase in hole density.

To fit the experimental data in Fig. 1(a), we have used as free parameters: P_C ; the strength of the barrier, Z ; the SC energy gap, Δ ; and T^* and infer the SP of about 90%, consistent with the other values reported in literature and a reduction of the SC energy gap. We underline that using the BTK model requires a very high effective temperature, $T^* = 10.95\text{K}$, which is more than 5 times the measured temperature of 1.9 K. According to [18], this effective temperature accounts for inelastic scattering in the (Ga,Mn)As sample, but in any case it is a parameter introduced "ad hoc", and whether such a high value of T^* can be justified on this basis is not clear¹⁹.

Recently, a theoretical model was introduced which allows for a more realistic description of interface scattering in the calculation of charge and spin transport across such point contacts^{14,20}. When a contact with a magnetic material is created, one would expect that the scattering properties of quasiparticles depend on their spin. When no tunneling potential is present, the transparency of the interface is controlled by wave vector mismatches. Since wave vectors of \uparrow - and \downarrow -spin quasiparticles are different in the FM material, their transmission probabilities should differ accordingly. Moreover, it was shown that scattering phases can play an important role in this case²¹. While a global phase will never affect any physical properties, the relative phase difference, that quasiparticles incident from the SC may acquire upon being reflected at the magnetic interface, induces a triplet proximity effect and leads to substantial modifications of conductance spectra¹⁴. This relative scattering phase is called *spin-mixing angle* or spin-dependent interface phase shift. In the case of point-contacts, it suppresses the coherence peaks at the gap-edge and shifts their spectral weight to energies below the gap, where interface Andreev bound states are induced. This mechanism allows for an alternative interpretation of the PCAR spectra analyzed here. Using a minimal model of spin-active scattering (SAS), we show that excellent fits can be achieved without resorting to the effective T^* .

The transport theory proposed in Ref.¹⁴ relies on the normal-state scattering matrix of the interface as a phenomenological parameter. This S-matrix generally depends on the impact angle of the incident quasiparticles. We assume that spin-flip scattering due to spin-orbit coupling can be neglected (this approximation is appropriate for sufficiently strong SP), hence the S-matrix is diagonal in spin-space, yet

we allow for different transmission probabilities $t_\uparrow \neq t_\downarrow$ and a spin-mixing angle ϑ . Since there is no insulating interlayer, we assume that the transmission probability is controlled by wave vector mismatches. We use the averaged Fermi wave vectors of the (Ga,Mn)As spin bands $k_{\uparrow,\downarrow}/k_{SC}$ as fit parameters. Here, k_{SC} is the Fermi wave vector in the SC. $t_\uparrow(\theta)$ and $t_\downarrow(\theta)$ are then calculated for any impact angle θ by wave function matching. The density of states $N_{\uparrow,\downarrow}$ (at Fermi energy E_F) of the respective spin-band is assumed to be proportional to $k_{\uparrow,\downarrow}$ and independent of energy on the relevant scale of the SC gap. The third parameter describing the interface is the spin-mixing angle ϑ which also depends on the impact angle. If the conduction bands of the materials are assumed to be unperturbed at the interface, this relative scattering phase will not occur. However, if the transition from one material to the other is smoothed on the scale of the Fermi-wavelength in Nb¹⁴, it will. We assume that this mixing phase is maximal for perpendicular impact and goes to zero for grazing trajectories. For definiteness, this is modeled by $\vartheta(\theta) = \vartheta \cdot \cos(\theta)$, but even if $\vartheta(\theta) = const$ is assumed, it does not change anything about our conclusions, since grazing trajectories contribute little to the total conductance. Additionally, the value of the SC gap and a spread resistance are fitted, while the temperature is taken from experiment. For details of the calculations involved we refer the reader to Ref.^{14,20}. In addition to ϑ , the fits in Fig. 1(b-d) using the SAS model involve Δ , k_\uparrow/k_{SC} , k_\downarrow/k_{SC} and R_s/R_{pc} as fit parameters. Here, the spread resistance R_s arises from the resistance of the sample between the junction and one of the measuring contacts⁸ renormalizing both the voltage that drops across the contact and the normalized conductance. The value of R_s/R_{pc} found by fitting (between 2.4 and 1.4 in Fig. 1 (b)–(d)) is rather high as the conductance of (Ga,Mn)As is low compared to metallic samples and it is likely that multiple shunted contacts are established when the tip is pressed into the sample. Spin-mixing angles are close to 0.5π in all cases. We also find a reduction of Δ , namely to $\approx 50\%$ with respect to the zero temperature bulk value, reported to be 1.5 meV in Nb for the lowest temperature spectra we measured. Judging by the disappearance of all SC features, T_c is reduced to 5.4 – 5.8 K. This implies a deviation from the theoretical strong-coupling BCS ratio²² for Nb ($2\Delta/k_B T_C \approx 3.95$), instead we find $2\Delta/k_B T_C \approx (3.3 \pm 0.3)$. The fitting for different temperatures at the same measurement location was done by only varying Δ , all other parameters are kept constant. Remarkably, the quality of the fits for all temperatures in Fig. 2 is still very good and rescaling the obtained gap values to the BCS relation also yields a satisfactory agreement, see inset of Fig. 2. The strong reduction of the gap could indicate that an inverse proximity effect may be important.

Wavevectors inferred from the fits in Fig. 1(b)–(d) vary little around $k_\uparrow/k_{SC} = 0.447$ and $k_\downarrow/k_{SC} = 0.237$. Based on the assumptions of our model^{14,20}, the transport SP

$$P_C = 2 [\langle s_z v \rangle_\uparrow + \langle s_z v \rangle_\downarrow] / [\langle v \rangle_\uparrow + \langle v \rangle_\downarrow], \quad (1)$$

can be expressed as $P_C \approx (1 - r^2)/(1 + r^2)$ with $r = k_\downarrow/k_\uparrow$, provided that the effective masses in both spin-bands $\{\uparrow, \downarrow\}$ are approximately the same. In the Fermi-surface averages

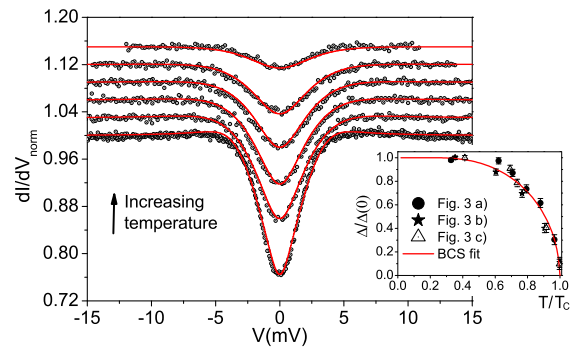


FIG. 2: (Color online) Spectra as a function of temperature (black dots) with the theoretical fittings obtained by considering the spin-mixing effect with the energy gap as only free parameter. Spectra are shifted and shown for temperatures between 1.9 K and 5.6 K. Inset: Temperature dependence of the superconducting energy gap as found from the theoretical fittings rescaled to the BCS relation.

$\langle f \rangle_i \equiv \int d^3k f(\vec{k}) \delta(E_F - \varepsilon_{\vec{k},i})$, we consider v and s_z that are the group velocities $(1/\hbar)|\nabla_k \varepsilon_{\vec{k},i}|$ and the spin expectation value projected to the direction of magnetization (taken to be z here). $\varepsilon_{\vec{k},i}$ are the band dispersions and E_F is the Fermi level. In the following, we comment on two particular aspects of the values of P_C deduced from the PCAR spectra: (i) our annealed and as-grown samples lead us, within experimental error, to the same value of P_C which (ii) is significantly lower than previously assumed based on the BTK theory. We explain these findings in the framework of the warped six-band $\vec{k} \cdot \vec{p}$ model with mean field kinetic-exchange due to Mn²³. It allows us to evaluate an estimate for P_C in Eq. (1) (extended to six bands) using essentially two parameters: E_F and FM splitting h . In Fig. 3(a) we recast the former into the total carrier (hole) concentration p for convenience while the latter is a product of N_{Mn} , concentration of Mn moments that participate in the FM order, Mn total spin $S_{Mn} = \frac{5}{2}$ and the Mn-hole exchange J_{pd} . Points labelled 'G' (as-grown) and 'A' (annealed) correspond to h determined from the commonly accepted value²⁴ of $J_{pd} = 55 \text{ meV} \cdot \text{nm}^3$ and the remanent magnetization at low temperatures ($T \ll T_C$) as measured by SQUID magnetometry for the as-grown and annealed sample, respectively²⁵. Addressing the points (i) and (ii) above, we note that P_C has nearly equal values in 'G' and 'A' and these values are rather low. In particular, (i) the increase of hole concentration upon annealing (as also witnessed by the drop of p) is compensated for by an increase of the FM splitting which may result in practically unchanged P_C after annealing; the values $P_C \approx 0.38$ and 0.31 ('G' and 'A' in Fig. 3(a)) should be viewed as equal within the experimental uncertainty of $\Delta p = 0.2 \text{ nm}^{-3}$ (hole concentration is not precisely known as other compensation mechanisms than interstitial Mn²⁵ may be at work). Next, (ii) although we do not attempt an accurate quantitative comparison between the theoretically estimated P_C and the PCAR-inferred values, most importantly we find that it is impossible to obtain values of polarization approaching 90% from the $\vec{k} \cdot \vec{p}$ + exchange model for reasonable hole and moment densities for our material. The remaining dis-

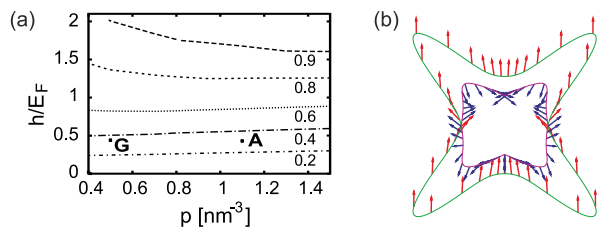


FIG. 3: (Color online) The $\vec{k} \cdot \vec{p}$ model of (Ga,Mn)As²³ used to evaluate (a) total P_C calculated by generalizing Eq. (1) to all six bands involved (only isolines of P_C are shown) and (b) expectation values of spin (spin-textures) in the heavy-hole bands at the Fermi surface (k_y, k_z section is shown; $\hbar = 165$ meV, $p = 0.8$ nm⁻³). Note that, while the z -component of spin is not a good quantum number, the two bands can still be approximately labeled as "up" (majority) and "down" (minority).

crepancy between the $\vec{k} \cdot \vec{p}$ ($P_C \approx 35\%$) and the SAS models ($P_C \approx 57 \pm 2\%$, Fig. 1(b-d)) may have its origin on either side. The value of J_{pd} could be in fact somehow larger thus shifting the points 'A' and 'G' upwards in Fig. 3(a). Also, the precise role of impurity scattering in the strongly doped materials has not been elucidated so far.²⁶ Alternatively, the SAS model could be refined to account for non-spherical bands that entail appreciable spin-orbit interaction. As exemplified in Fig. 3(b), both these effects are significant in (Ga,Mn)As. Nevertheless, even with these imperfections, the combined results of the SAS analysis of the PCAR data and the $\vec{k} \cdot \vec{p}$ model provide convincing evidence that the transport SP in typical

high- T_C (Ga,Mn)As sample is significantly less than 100%.

We have studied the transport spin-polarization at the Fermi level in (Ga,Mn)As with the PCAR technique, using a recently developed theory that accounts for spin-active scattering at the interface to model the experimental results. Compared to previous work on PCAR with this material, this allowed us to drop the assumption of an effective temperature. The value of the SP we obtain from this analysis is sizeable but significantly smaller than that inferred by earlier studies and it now agrees better with predictions of the $\vec{k} \cdot \vec{p}$ kinetic-exchange model of (Ga,Mn)As. We also investigated the full temperature dependence of the spectra and find a strong suppression of the SC gap. The temperature dependence of the fitted gap values is in agreement with the BCS relation. Our study paves the way for further investigations to improve the understanding of transport mechanisms that occur at SC/FM-semiconductor interfaces, whose satisfactory characterization stands as a topic of central interest both for fundamental physics and for technological applications in spintronics. The results of this paper are likely to stimulate a critical reassessment of previous literature where the spin-active mechanism was incompletely modeled leading to unreliable estimates of SP of such materials.

We thank L. Cohen, T. Jungwirth, K. Yates, M. Humphry, and L. Kripner for discussions and support. Funding from the EU (Grants NAMASTE-214499 and SemiSpinNano-237375) and from the ASCR (GA AV Contract KJB100100802 and Præmium Academiæ) is acknowledged.

- ¹ S. A. Wolf, *et al.*, *Science* **294**, 1488 (2001).
- ² D. D. Awschalom, and M. E. Flatté, *Nature Phys.* **3**, 153 (2007).
- ³ T. Jungwirth, *et al.*, *Rev. Mod. Phys.* **78**, 809 (2006).
- ⁴ V. Novák, *et al.*, *Phys. Rev. Lett.* **101**, 077201 (2008); M. Wang, *et al.*, *Appl. Phys. Lett.* **93**, 132103 (2008).
- ⁵ Y. Ohno, *et al.*, *Nature* **402**, 790 (1999).
- ⁶ C. Adelman, *et al.*, *J. Vac. Sci. Tech. B* **23**, 1747 (2005).
- ⁷ R. Meservey, P. M. Tedrow, *Phys. Rep.* **238**, 173 (1994).
- ⁸ G. T. Woods, *et al.*, *Phys. Rev. B* **70**, 054416 (2004).
- ⁹ M. J. M. de Jong and C. W. J. Beenakker, *Phys. Rev. Lett.* **74**, 1657 (1995).
- ¹⁰ R.J. Soulen Jr., *et al.*, *Science* **282**, 85 (1998).
- ¹¹ I. I. Mazin, A. A. Golubov, and B. Nadgorny, *J. Appl. Phys.* **89**, 7576 (2001).
- ¹² G. J. Strijkers, *et al.*, *Phys. Rev. B* **63**, 104510 (2001).
- ¹³ G. E. Blonder, M. Tinkham, and T. M. Klapwijk, *Phys. Rev. B* **25**, 4515 (1982).
- ¹⁴ R. Grein *et al.*, *Phys. Rev. B* **81**, 094508 (2010).
- ¹⁵ K. Xia *et al.*, *Phys. Rev. Lett.* **89**, 166603 (2002); F. Taddei *et al.*, *J. Low Temp. Phys.* **124**, 305 (2001).
- ¹⁶ A. Geresdi, *et al.*, *Phys. Rev. B* **77**, 233304 (2008).
- ¹⁷ R.P. Campion, *et al.*, *J. Cryst. Growth* **247**, 42 (2003).
- ¹⁸ R. P. Panguluri, *et al.*, *Phys. Rev. B* **72**, 054510 (2005).
- ¹⁹ Letting a $\Gamma_{\text{Dynes}} \neq 0$ parameter in the fitting model [R.C. Dynes *et al.*, *Phys. Rev. Lett.* **41**, 1509 (1978)], it would add to the smear-out of the spectrum allowing for a smaller T^* , yet Γ_{Dynes} describes a finite quasiparticle lifetime in the SC (not in the FM) material. As the incongruences in BTK fits are related to the (Ga,Mn)As sample rather than the Nb tip, it would be improper to regard a Nb bulk property as a possible explanation.
- ²⁰ M. Eschrig, *Phys. Rev. B* **80**, 134511 (2009).
- ²¹ M. Eschrig and T. Löfwander, *Nat. Phys.* **4**, 138 (2008).
- ²² F. Marsiglio and J. P. Carbotte, *Phys. Rev. B* **33**, 6141 (1986).
- ²³ M. Abolfath *et al.*, *Phys. Rev. B* **63**, 054418 (2001).
- ²⁴ J. Okabayashi *et al.*, *Phys. Rev. B* **58**, R4211 (1998).
- ²⁵ p was determined by assuming that N_{Mn} corresponds to substitutional Mn (single acceptor) while the remaining Mn in the as-grown sample (as given by the nominal doping of 7%) stay in interstitial positions where each Mn acts as a double donor. Upon annealing, all interstitials are removed. Used values of N_{Mn} and p agree well with previous characterization studies such as K.Y. Wang *et al.*, *J. Appl. Phys.* **95**, 6512 (2004) or T. Jungwirth, *et al.*, *Phys. Rev. B* **72**, 165204 (2005).
- ²⁶ J. Mašek *et al.*, *Phys. Rev. Lett.* **105**, 227202 (2010).